Supplementary Information

Synaptotagmin IV determines the linear Ca^{2+} dependence of vesicle fusion at auditory ribbon synapses

Stuart L. Johnson, Christoph Franz, Stephanie Kuhn, David N. Furness, Lukas Rüttiger, Stefan Münkner, Marcelo N. Rivolta, Elizabeth P. Seward, Harvey R. Herschman, Jutta Engel, Marlies Knipper and Walter Marcotti

This document includes seven Supplementary Figures with legends, two Supplementary Tables and a Reference list.

Nature Neuroscience: doi:10.1038/nn.2456

Supplementary Figure 1

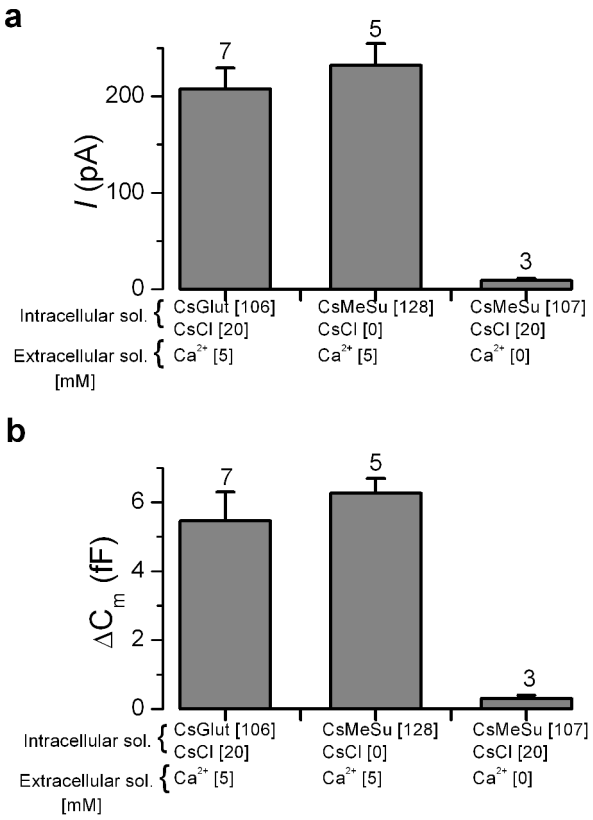

Supplementary Figure 1. Ca^{2+}-induced ΔC_m measurements were not contaminated with non-linear capacitance in early postnatal OHCs from control Syt IV mice.

Current evidence indicates that the onset of electromotile activity in mouse OHCs occurs at around the end of the first postnatal week[1]. However, we tested whether a possible early onset of this activity in Syt IV control mice (P3–P4) could affect our ΔC_m measurements by manipulating the intracellular and extracellular recording solutions.

Average maximal values of I_{Ca} (**a**) and ΔC_m (**b**) from control Syt IV OHCs in normal experimental conditions (left columns are data from **Fig. 3** of the main text) were compared to those obtained using different intracellular anionic compositions, known to affect the OHC motor's voltage-sensor charge movement. When Cs-Glutamate (CsGlu) and CsCl were exchanged for Cs-MethaneSulphonate (CsMeSu), which significantly attenuates the electromotile activity[2], I_{Ca} and ΔC_m values were not affected. We also verified that our ΔC_m measurements were mainly driven by Ca^{2+} and not by OHC motility by superfusing a Ca^{2+}-free extracellular solution (0 CaCl plus 0.5 mM EGTA). Both I_{Ca} and ΔC_m were almost completely abolished in the absence of Ca^{2+}, similar to previous results obtained in the non-electromotile IHCs[3]. Experiments were performed as described in **Fig. 3** of the main text.

Supplementary Figure 2

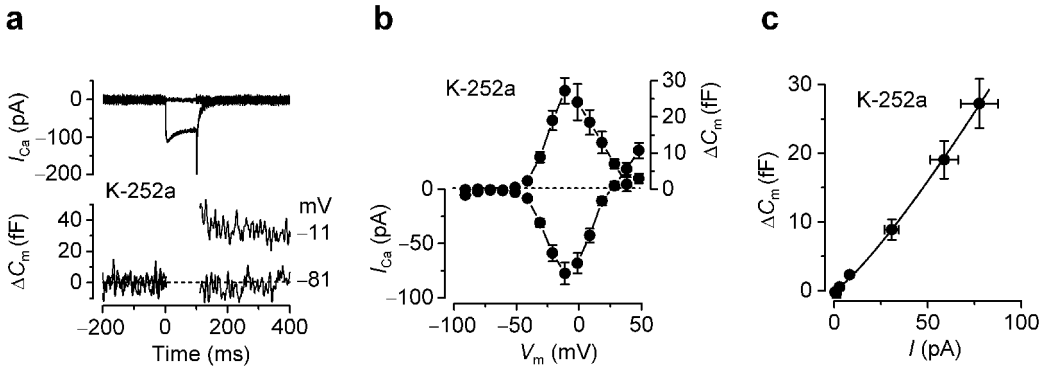

Supplementary Figure 2. The linear exocytotic Ca^{2+} dependence of adult IHCs is not affected by K-252a.

Neurotrophins such as brain-derived neurotrophic factor (BDNF) have been shown to affect synaptic transmission in the CNS[4,5]. A recent study on cultured hippocampal neurons has shown that Syt IV is specifically associated with BDNF containing vesicles and functions to inhibit retrograde BDNF release onto the presynaptic site thereby indirectly reducing synaptic transmission[6].

In order to investigate whether the linear Ca^{2+} dependence of exocytosis in adult IHCs results from retrograde Syt IV mediated BDNF signalling we perfused the cells with K-252a, an inhibitor of tyrosine kinase receptors[7] that blocks the activity of BDNF[5, 8].

Calcium currents and exocytosis were recorded from IHCs (n = 8) of P18 Syt IV control mice. K-252a (10 μM; Sigma) was bath-applied onto IHCs for at least 20 mins (ranging up to 45 mins) before patch-clamping, and then maintained throughout recording. **(a)** I_{Ca} and ΔC_m recordings in response to the same protocol described in **Fig. 1a** but in the presence of K-252a. **(b)** I_{Ca}-V and ΔC_m-V curves showing a normal maximal I_{Ca} (−78 ± 10 pA) and ΔC_m (27 ± 4 fF). **(c)** the synaptic transfer relation, obtained as described in **Fig. 1c**, was normal in the presence of K-252a. The average N value from fits to all individual cells was 1.3 ± 0.1 (not significantly different from the value obtained for control cells in **Fig. 1c**).

Supplementary Figure 3

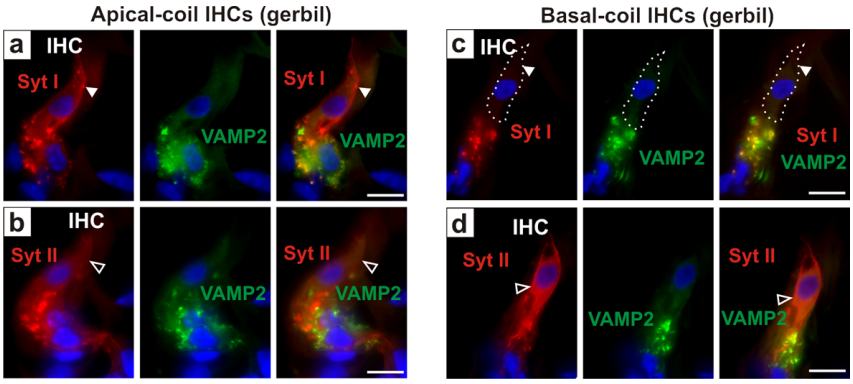

Supplementary Figure 3: Synaptotagmin I and II immunolabelling in apical- and basal-coil IHCs from the adult gerbil.

Syt I (**a**, red) and Syt II (**b**, red) stained IHCs from the apical-coil of the adult (P17) gerbil cochlea. Note that Syt II labelling was considerably weaker in the IHC but not in the region of the efferent fibres (VAMP2 was used as an efferent marker: green). Comparison of Syt I (**c**) and Syt II (**d**) protein staining in the basal region of the adult gerbil cochlea. As shown for the mouse, Syt I was selectively expressed in the efferent fibres and Syt II in both IHCs and efferents. Scale bars indicate 10 µm.

Supplementary Figure 4

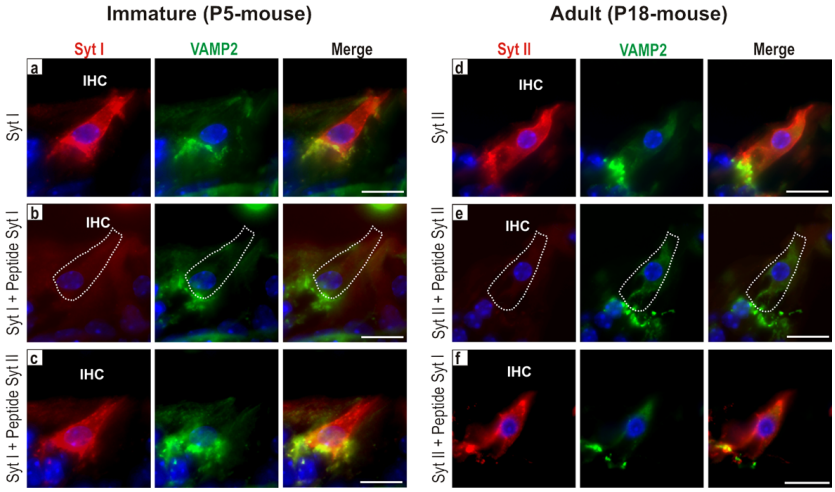

Supplementary Figure 4. Specificity of synaptotagmin I and II labelling.

(**a**–**c**), The specificity of Syt I antibody staining in the IHC region of the immature mouse. Syt I was present in IHCs (**a**, red) and in the efferent fibres (**a**, green) as shown by the double-labelling with the efferent marker VAMP2 (**a**, merge). Syt I fluorescence was not detected when the Syt I antibody was pre-incubated together with the Syt I peptide (**b**). The incubation of Syt I antibody with the Syt II specific peptide did not lead to a loss of protein staining in the IHC or efferent fibres (**c**). (**d**–**f**), Syt II staining in the adult (P18) mouse cochlea was present at the level of the IHC and efferent fibres (**d**). When the Syt II antibody was incubated with its peptide no Syt II fluorescence signal could be detected (**e**). Syt II staining was still present when the antibody was incubated with the Syt I specific peptide (**f**). Images are single layer and the scale bars indicate 10 µm.

Supplementary Figure 5

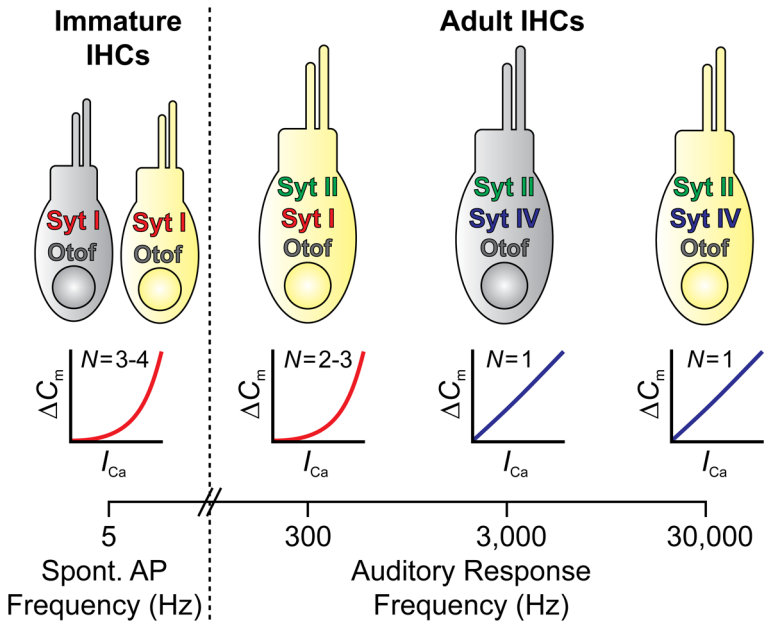

Supplementary Figure 5. Diagram showing the correlation between the distribution of synaptotagmins and the exocytotic Ca^{2+} dependence in mammalian IHCs.

The expression of synaptotagmins (Syts) and otoferlin (Otof) in immature and adult mouse (grey) and gerbil (yellow) IHCs. Immature IHCs fire spontaneous action potentials (APs) at about 5 Hz[9], express Syt I and show a high-order exocytotic Ca^{2+} dependence. In adult animals, the auditory frequency range differs depending on the species (mouse: ~2–80 kHz; gerbil: ~0.1–60 kHz), such that the low-frequency region of the gerbil (shown as ~300 Hz) is considerably lower than that of the mouse (~3,000 Hz). These differences are represented in the characteristic physiological responses generated by IHCs, such that the receptor potentials from the higher frequency cells (>~1,500 Hz) consist of a sustained component that is graded to represent sound intensity whereas those of low-frequency IHCs are mainly composed of a phasic component (somewhat similar to immature IHC AP activity) that follows the sound frequency.

The phasic or sustained components of the IHC receptor potential are likely to be emphasized by the high-order or linear exocytotic Ca^{2+} dependence, respectively[10]. Low-frequency "phasic" IHCs (immature and adult apical gerbil cells) express Syt I while "sustained" cells express Syt IV (adult apical mouse [3,000 Hz] and basal gerbil IHCs [30,000 Hz]). Note that currently there are no published data on high-frequency [80,000 Hz] adult mouse IHCs. Syt II expression seems to be a characteristic of adult IHCs. Otoferlin, the other known Ca^{2+} sensor involved in cochlear hair cell exocytosis[11,12], is expressed in all IHCs throughout development[10–13]. Current evidence suggests that otoferlin is likely to be essential for the topographical organization of the synaptic active zones[14] and synaptic vesicle pool replenishment[14] (see also **Fig. 6f**).

Supplementary Figure 6

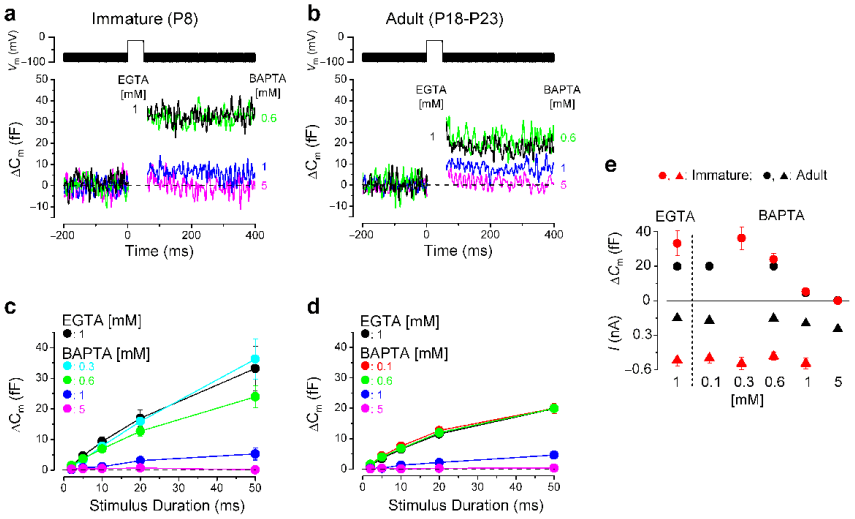

Supplementary Figure 6. Effect of Ca^{2+} buffering on RRP release in immature and adult mouse IHCs.

The release of each docked vesicle at the IHC presynaptic membrane is controlled by a nearby cluster of Ca^{2+} channels. Differences in the relative distance between Ca^{2+} channels and the readily releasable pool (RRP) of vesicles could determine/influence the Ca^{2+} dependence of neurotransmitter release. Therefore, we estimated this spatial distance in immature and adult IHCs by measuring synaptic vesicle exocytosis whilst using either intracellular EGTA (1 mM) or different BAPTA concentrations, a Ca^{2+} chelator with faster binding kinetics than EGTA and therefore capable of buffering Ca^{2+} elevations closer to their source[15].

ΔC_m was induced by the activation of I_{Ca} in response to a depolarizing voltage step from –81 mV to near –11 mV (**a** and **b**) and the stimulus duration was varied over a sufficiently short range to isolate the RRP (from 2 ms to 50 ms: **c** and **d**; see also refs. 3,9). While I_{Ca} was relatively unaffected by the Ca^{2+} buffer, the exocytotic machinery and Ca^{2+} channels were significantly uncoupled in the presence of 1 mM BAPTA in IHCs from both age ranges (**e**: immature: $P < 0.01$ when compared to either EGTA or 0.3 mM BAPTA and $P < 0.05$ with 0.6 mM BAPTA; adult: $P < 0.001$ when compared to EGTA or 0.1 and 0.6 mM BAPTA). The space constant in the presence of 2 mM BAPTA is estimated to be 28 nm[16]. Therefore, the space constant for 1 mM BAPTA would be about √2 greater (see eqn (2) in ref. 15), indicating that, vesicles of the RRP in mouse IHCs are likely to be localized in the order of 40 nm from Ca^{2+} channels irrespective of the stage of development. A similar finding has been shown for gerbil IHCs[10,13]. The similar spatial coupling observed for immature and adult IHCs excludes that their different exocytotic Ca^{2+} dependence is caused by a different spacing between Ca^{2+} channels and ribbons. Number of cells are: apical 4 (EGTA); 3, 5, 4, 4 (BAPTA). Basal 4; 3, 3, 6, 3.

Supplementary Figure 7

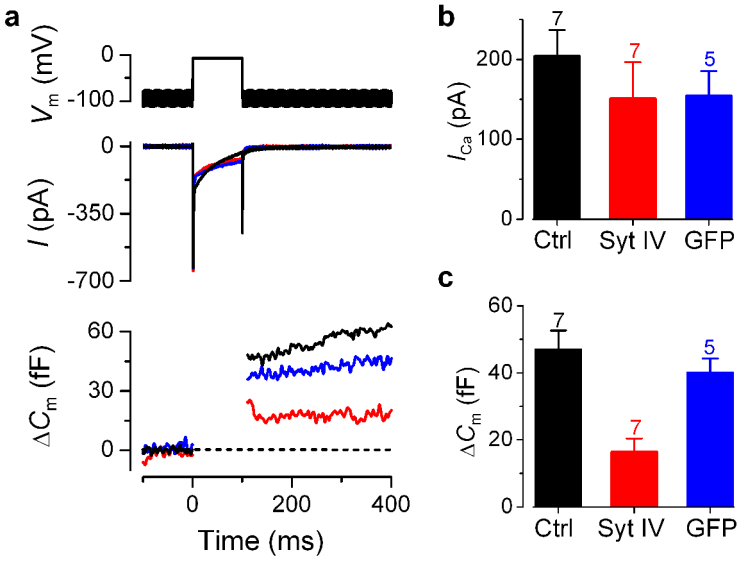

Supplementary Figure 7. Ca^{2+}-triggered exocytosis in adult bovine chromaffin cells expressing Syt IV or GFP.

We investigated the effect of expressing Syt IV on exocytosis in adult bovine chromaffin cells prepared as described previously[17] and transfected by electroporation[18]. Like immature IHCs, chromaffin cells utilize Syt I as the endogenous Ca^{2+} sensor for triggering fast exocytosis and do not express Syt II.

Data presented in **a**–**c** summarizes the effect of expressing Syt IV with GFP or GFP only (used as a transfection control) on Ca^{2+}-triggered exocytosis in adult bovine chromaffin cells. All solutions used to measure I_{Ca} and ΔC_m were as described previously[19]. Secretion was triggered by stepping the membrane potential from –90 to 0 mV for 100 ms (**a**: traces are average from all cell tested), 300 ms or 1 s (data not shown). Exocytosis evoked by the 100–300 ms depolarizing steps is dominated by release from the RRP, while the longer depolarization also recruits release from the slowly releasable pool of vesicles. Compared with the GFP expressing or mock transfected cells, the expression of Syt IV significantly reduced exocytosis from the RRP (**c**: $P < 0.001$) without changing calcium entry (**b**). This finding supports a previous observation in PC12 cells using an immunofluorescence assay[20]. When the longer pulse duration (1 s) was used on chromaffin cells, the effect of Syt IV expression was to reduce total secretion but not significantly from that in control cells (data not shown), suggesting that Syt IV does not interact with the Ca^{2+} sensor used in slow secretion in these cells, recently identified as Syt VII[21]. These findings support the notion Syt IV can interact with other Syt isoforms to alter the Ca^{2+} dependence of exocytosis, but that the nature of the interaction may be isoform-specific and that in the case of Syt I this leads to a decrease in exocytotic efficiency. This latter observation could explain the importance of a switch from Syt I to Syt II in IHCs.

Supplementary Table 1

Supplementary Table 1. Biophysical properties of immature IHCs from Syt IV mice.

	Control (P5, n = 8)	Knockout (P5, n = 6)
Membrane capacitance (pF)	7.7 ± 0.3	8.2 ± 0.3
Resting potential (mV)	–52.0 ± 1.1	–52.0 ± 0.4
g_{leak} (nS)	3.2 ± 0.4	3.7 ± 0.1
$I_{K,neo}$ at 0 mV (nA)	5.2 ± 0.3	5.2 ± 0.7

Values are means ± s.e.m. $I_{K,neo}$ is a delayed rectifier K^+ current[22]. In knockouts, the resting membrane potential value was obtained from 4 IHCs. All values shown above were found not to be significantly different between control and knockout IHCs. Immature IHCs also showed normal expression of additional K^+ currents characteristic of these cells (I_{SK}: ref 23; I_{K1}: ref 24; data not shown).

Supplementary Table 2

Supplementary Table 2. Biophysical properties of adult IHCs from Syt IV mice.

	Control (P28, n = 7)	Knockout (P29, n = 7)
Membrane capacitance (pF)	10.1 ± 0.4	9.9 ± 0.4
Resting potential (mV)	–67 ± 2	–72 ± 2
g_{leak} (nS)	0.4 ± 0.1	0.3 ± 0.1
g_{slope} at –74 mV (nS)	6.0 ± 0.6	6.3 ± 0.5
$I_{K,n}$ at –124 mV (pA)	–202 ± 26	–249 ± 19
$I_{K,f}$ at –25 mV (nA)	2.7 ± 0.3	3.2 ± 0.7
I_K at 0 mV (nA)	12 ± 1	16 ± 1

Values are means ± s.e.m. $I_{K,n}$ is a negatively activating delayed rectifier K^+ current[22]. I_K represents the combination of both the BK current $I_{K,f}$ and a classical delayed rectifier $I_{K,s}$ (ref. 25). Isolated $I_{K,f}$ and $I_{K,n}$ were measured as previously described[22,25]. All values shown above were found not to be significantly different between control and knockout IHCs.

References

1. Abe, T., Kakehata, S., Kitani, R., Maruya, S., Navaratnam, D., Santos-Sacchi, J. & Shinkawa, H. Developmental expression of the outer hair cell motor prestin in the mouse. *J. Membr. Biol.* **215**, 49-56 (2007).
2. Rybalchenko, V. and Santos-Sacchi, J. Anion control of voltage sensing by the motor protein prestin in outer hair cells. *Biophys. J.* **95**, 4439-4447 (2008).
3. Johnson, S.L., Marcotti, W. & Kros, C.J. Increase in efficiency and reduction in Ca^{2+} dependence of exocytosis during development of mouse inner hair cells. *J. Physiol.* **563**, 177-191 (2005).
4. Lu, B. BDNF and activity-dependent synaptic modulation. *Learn. Mem.* **10**, 86-98 (2003).
5. Madara, J.C. & Levine, E.S. Presynaptic and postsynaptic NMDA receptors mediate distinct effects of brain-derived neurotrophic factor on synaptic transmission. *J. Neurophysiol.* **100**, 3175-3184 (2008).
6. Dean, C., Liu, H., Dunning, F.M., Chang, P.Y., Jackson, M.B. & Chapman, E.R. Synaptotagmin-IV modulates synaptic function and long-term potentiation by regulating BDNF release. *Nat. Neurosci.* **12**, 767-776 (2009).
7. Knüsel, B. & Hefti, F. K-252 compounds: modulators of neurotrophin signal transduction. *J. Neurochem.* **59**, 1987-1996 (1992).
8. Levine, E.S., Dreyfus, C.F., Black, I.B. & Plummer, M.R. Brain-derived neurotrophic factor rapidly enhances synaptic transmission in hippocampal neurons via postsynaptic tyrosine kinase receptors. *Proc Natl Acad Sci USA* **92**, 8074-8077 (1995).
9. Johnson. S.L., Adelman, J.P. & Marcotti, W. Genetic deletion of SK2 channels in mouse inner hair cells prevents the developmental linearization in the Ca^{2+} dependence of exocytosis. *J. Physiol.* **583**, 631-646 (2007).
10. Johnson, S.L., Forge, A., Knipper, M., Münkner, S. & Marcotti, W. Tonotopic variation in the calcium dependence of neurotransmitter release and vesicle pool replenishment at mammalian auditory ribbon synapses. *J. Neurosci.* **28**, 7670-7678 (2008).
11. Roux, I. *et al.* Otoferlin, defective in a human deafness form, is essential for exocytosis at the auditory ribbon synapse. *Cell* **127**, 277-289 (2006).
12. Beurg, M. *et al.* Calcium- and otoferlin-dependent exocytosis by immature outer hair cells. *J. Neurosci.* **28**, 1798-1803 (2008).
13. Johnson, S.L., Franz, C., Knipper, M. & Marcotti W. Functional maturation of the exocytotic machinery at gerbil hair cell ribbon synapses. *J. Physiol.* **587**, 1715-1726 (2009).
14. Heidrych, P. *et al.* Otoferlin interacts with myosin VI: implications for maintenance of the basolateral synaptic structure of the inner hair cell. *Hum. Mol. Genet.* **18**, 2779-2790 (2009).
15. Neher, E. Vesicle pools and Ca^{2+} microdomains: new tools for understanding their roles in neurotransmitter release. *Neuron* **20**, 389-399 (1998).
16. Naraghi, M. & Neher, E. Linearized buffered Ca^{2+} diffusion in microdomains and its implications for calculation of $[Ca^{2+}]$ at the mouth of a calcium channel. *J. Neurosci.* **17**, 6961-6973 (1997).
17. Bauer, C.S., Woolley, R.J., Teschemacher, A.G. & Seward, E.P. Potentiation of exocytosis by phospholipase C-coupled G-protein-coupled receptors requires the priming protein Munc13-1. *J. Neurosci.* **27**, 212-219 (2007).
18. Weiss, J.L. & Burgoyne, R.D. Voltage-independent inhibition of P/Q-type Ca2+ channels in adrenal chromaffin cells via a neuronal Ca2+ sensor-1-dependent pathway involves Src family tyrosine kinase. *J Biol.Chem.* **276**, 44804-44811 (2001).

19. Seward, E.P. & Nowycky, M.C. Kinetics of stimulus-coupled secretion in dialyzed bovine chromaffin cells in response to trains of depolarizing pulses. *J. Neurosci.* **16**, 553-562 (1996).
20. Machado, H.B., Liu, W., Vician, L.J. & Herschman, H.R. Synaptotagmin IV overexpression inhibits depolarization-induced exocytosis in PC12 cells. *J. Neurosci. Res.* **76**, 334-341 (2004).
21. Schonn, J.S., Maximov, A., Lao, Y., Sudhof, T.C. & Sorensen, J.B. Synaptotagmin-1 and -7 are functionally overlapping Ca2+ sensors for exocytosis in adrenal chromaffin cells. *Proc. Natl. Acad. Sci. USA* **105**, 3998-4003 (2008).
22. Marcotti, W., Johnson, S.L., Holley, M.C. & Kros, C.J. Developmental changes in the expression of potassium currents of embryonic, neonatal and mature mouse inner hair cells. *J. Physiol.* **548**, 383-400 (2003).
23. Marcotti, W., Johnson, S.L. & Kros, C.J. A transiently expressed SK current sustains and modulates action potential activity in immature mouse inner hair cells. *J. Physiol.* **560**, 691-708 (2004b).
24. Marcotti, W., Géléoc, G.S.G., Lennan, G.W.T. & Kros, C.J. Developmental expression of an inwardly rectifying potassium conductance in inner and outer hair cells along the mouse cochlea. *Pflügers Arch.* **439**, 113-122 (1999).
25. Marcotti, W., Johnson, S.L. & Kros, C.J. Effects of intracellular stores and extracellular Ca^{2+} on Ca^{2+}-activated K^{+} currents in mature mouse inner hair cells. *J. Physiol.* **557**, 613-633 (2004a).